AMERICAN JOURNAL OF PHYSICAL ANTHROPOLOGY 109:67–88 (1999)

A Model of Temporomandibular Joint Function in Anthropoid Primates Based on Condylar Movements During Mastication

CHRISTINE E. WALL*
Department of Biological Anthropology and Anatomy, Duke University Medical Center, Durham, North Carolina 27710

KEY WORDS mandible; temporomandibular joint; kinematics; diet

ABSTRACT The hypothesis that the shape of the bony temporomandibular joint (TMJ) is functionally related to sagittal sliding of the condyle during mastication is tested, and a model of the relation of sagittal sliding to mandibular size, TMJ shape, and diet is developed. Sagittal sliding is defined as fore-aft motion of the condyle during mandibular translation and/or angular rotation. Ascending ramus height is used as a structural correlate of the distance between the condyle and the mandibular axis of rotation (CR). Cineradiographic data on sagittal sliding and gape during mastication in *Ateles* spp., *Macaca fascicularis*, *Papio anubis*, and *Pan troglodytes* in conjunction with comparative data on mandibular size and TMJ shape are used to evaluate the hypothesis. The results show that 1) linear and angular gape are highly positively correlated with sagittal sliding, 2) pure mandibular translation is rare during mastication, 3) the CR is rarely if ever located at the condyle during mastication, 4) angular gape should be standardized in interindividual comparisons of sagittal sliding, and 5) the height of the ascending ramus (and by inference the CR-to-condyle distance) is highly positively correlated with absolute sagittal sliding.

Sagittal sliding relative to the length of the articular eminence was the variable used to explore the relation between TMJ shape and sliding. This variable standardized absolute sagittal sliding relative to joint size. The relative depth and orientation of the articular eminence were not correlated with relative sagittal sliding. The anteroposterior curvature of the condyle was highly negatively correlated with relative sagittal sliding. Flat condyles are associated with large amounts of relative sagittal sliding. A flat condyle increases joint contact area, which reduces joint stress. A flat condyle also increases joint congruence, and this may facilitate the combined sliding and rolling motion of the condyle when the sliding motion is relatively large. The shape of the entoglenoid process was also positively correlated with relative sagittal sliding. A relatively large entoglenoid process may help to guide sagittal sliding and prevent excessive mediolateral sliding of the condyle. The functional model makes a number of predictions about the correlations between food consistency and food object size, mandibular size, TMJ shape, and sagittal sliding of the condyle during mastication and incision. Am J Phys Anthropol 109:67–88, 1999.

The temporomandibular joint (TMJ) is the paired, synovial joint connecting the mandible to the cranium. The glenoid fossa and preglenoid plane on the temporal bone and the condyle of the mandible comprise the bony joint surfaces. Articular surfaces

Contract grant sponsor: NSF; Contract grant numbers: DBS-9209004, DBS-9215072; Contract grant sponsor: LSB Leakey Foundation.

*Correspondence to: Christine E. Wall, Department of Biological Anthropology and Anatomy, Box 3170, Duke University Medical Center, Durham, NC 27710.
E-mail: Christine_Wall@baa.mc.duke.edu

Received 13 April 1998; accepted 4 January 1999.

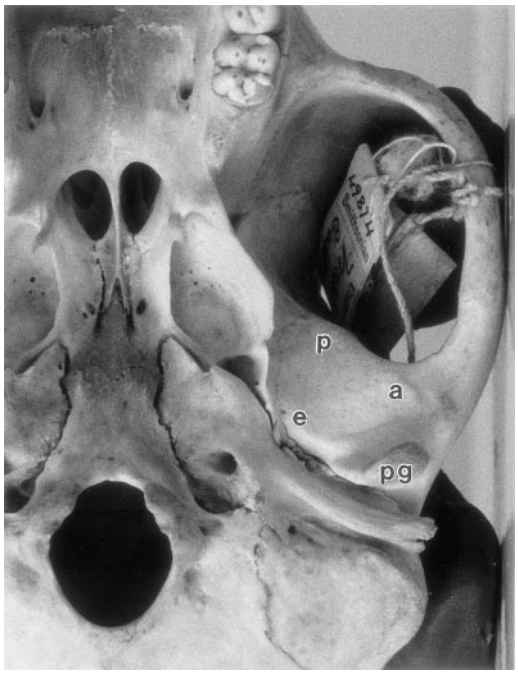

Fig. 1. Basicranial view of the left temporal articular surface of the TMJ (*Macaca nemestrina*, USNM 49874). The preglenoid plane extends anteriorly from the peak of the articular eminence. The entoglenoid process forms the medial boundary of the glenoid fossa. a, articular eminence; e, entoglenoid process; p, preglenoid plane; pg, postglenoid process.

are defined by the presence of articular tissue. The major articular surfaces of the TMJ are the articular eminence, the preglenoid plane, the entoglenoid process, and the head of the condyle. The articular eminence extends from the most superior point to the most inferior point of the glenoid fossa (Fig. 1). The preglenoid plane extends anteriorly from the most inferior point of the articular eminence to the insertion of the synovial capsule (Fig. 1). The capsular insertion raises a small bony ridge on the temporal bone. The entoglenoid process projects inferiorly from the medial side of the glenoid fossa (Fig. 1). In lateral view, the convex articular surface on the condyle has anterior, superior, and posterior aspects. Most of this articular surface is covered by a fibrocartilaginous articular disc that is firmly attached to the condylar head. Because of the great diversity in TMJ design seen among primates, the comparative anatomy of the TMJ has been important in taxonomic and functional conclusions about primate evolution (e.g., Keith, 1894; Parsons, 1900; Todd, 1930; Humphreys, 1932; Angel, 1948; Sicher, 1948; Robinson, 1952; Ashton and Zuckerman, 1954; Warwick James, 1960; DuBrul, 1977; Picq, 1990; Wall, 1997).

The primary functions of synovial joints are to facilitate movements while sustaining loads. Recent attention has focused on the implications of the joint reaction force for TMJ structure (e.g., Hylander, 1975, 1979a; Carlson et al., 1978, 1980; Hinton, 1981; Bouvier and Hylander, 1982; Bouvier, 1986a,b). By contrast, there are very little data available to evaluate the kinematic component of TMJ function and its relation to TMJ structure in nonhuman primates. In particular, the relation between sagittal sliding, kinematic parameters, and jaw structure is not well understood, and describing this relation in anthropoid primates is a major goal of this study. In describing this relation, a model of the kinematic component of TMJ function using cineradiographic and morphometric data is developed.

PURPOSE AND SCOPE OF THE STUDY

The hypothesis proposed here is that the shape of the bony TMJ, the amount of sagittal sliding during chewing, and the mechanical properties and size of food objects are interrelated functionally. This hypothesis is based on the assumptions that the TMJ has been shaped by natural selection to facilitate masticatory movements of the mandible. There is general agreement that some relation must exist between the shape of the bony TMJ and its movements (for recent reviews see Weijs and van Ruijven, 1990; Herring, 1992), but the extent of this relation is not known for primates. Similarly, it is logical to propose an association between diet and TMJ design because the TMJ has evolved to function under different dietary regimes. Morphometric data on TMJ shape and two-dimensional, cineradiographic data on condylar movements in a sample of anthropoid primates were analyzed in order to evaluate this hypothesis.

The disparity in the relative sizes of the temporal and condylar articular surfaces indicates that the anthropoid TMJ is highly

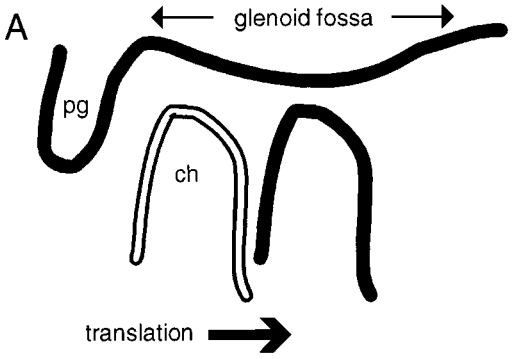

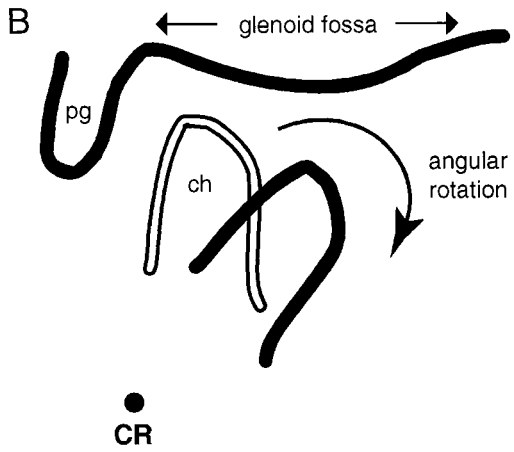

Fig. 2. Schematic, lateral view of the TMJ. ch, condyle; CR, axis of mandibular rotation; pg, postglenoid process, **A:** Movement of the condyle during mandibular translation. **B:** Movement of the condyle during angular rotation of the mandible about a transverse axis. Both types of movement cause sagittal sliding of the condyle relative to the glenoid fossa.

mobile. The temporal surface is much larger than the condylar surface. It is concave in places and convex in others (Fig. 1) but is generally much flatter than the condyle.

The movement of the mandible relative to the cranium can be described in terms of translation and angular rotation. As shown in Figure 2, both types of movement cause the condyle to slide. In addition, angular rotation causes the condyle to roll (Fig. 2B). Hylander et al. (1987) observed that in macaques intraindividual differences in sagittal sliding are positively correlated with linear gape and angular rotation (also referred to here as angular gape). The amount

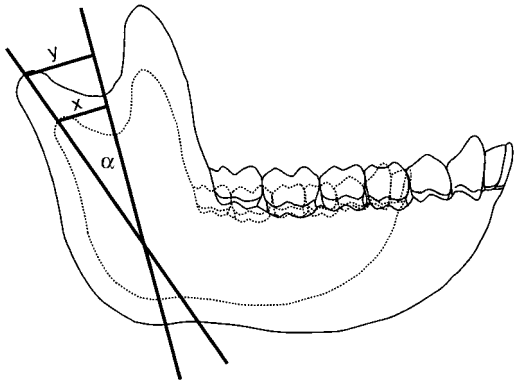

Fig. 3. A small mandible superimposed on a larger, geometrically scaled mandible. The ascending ramus is higher in the large mandible. The CR is in the same relative position in both mandibles. The amount of sagittal condylar sliding is greater in the large mandible (y) than in the small mandible (x) at an equivalent angular gape (in this case, 20°).

of sagittal sliding is also mechanically linked to and should therefore be correlated with the distance between the CR and the condyle (Fig. 3).

The extensive kinematic data on humans and the more limited data on nonhuman primates and other mammals indicate that the mandibular axis of rotation (the CR) is located at some distance from the condyle and that its location changes throughout both chewing and jaw open-close cycles (e.g., Bennett, 1908; Sheppard, 1962; Gibbs, 1969; Carlson, 1977; Weijs et al., 1989; Gallo et al., 1997). In support of these data, cineradiographic studies have shown that in nonhuman primates the condyle undergoes substantial sagittal sliding[1] during chewing (Hiiemae and Kay, 1973; Kay and Hiiemae, 1974a,b; Hylander and Crompton, 1980, 1986; Hylander et al., 1987; Jablonski and Crompton, 1994).

In this study, the height of the ascending ramus is used as a structural correlate of the position of the CR during mastication. Although it is preferable to measure its actual position, the determination of the CR loca-

[1]Sagittal sliding is the fore-aft movement of the condyle relative to the articular surface of the temporal bone. Sagittal sliding of a point on the condyle occurs during mandibular translation and during angular rotation of the mandible when the center of rotation is not coincident with the condylar point (Fig. 2).

tion from two-dimensional data incurs large computational errors (Panjabi, 1979).

The three-dimensional kinematic data indicate that the height of the ascending ramus is a reasonable structural correlate of the position of the CR. Gibbs (1969) and Gallo et al. (1997) described the location of the CR in humans from three-dimensional data during chewing and during jaw opening and closing, respectively. These studies show that the location of the CR varies and is rarely at the condyle. During a chewing cycle, the CR is frequently located inferior to the condyle, either within the ascending ramus, slightly inferior to the ascending ramus, posterior to the ascending ramus, or posterior and inferior to the ascending ramus (Gibbs, 1969). In general, these locations place the CR nearer to the lower border of the ascending ramus than to the condyle. As a result, the CR is near the insertions of the masseter and medial pterygoid muscles and the deep tendon of the anterior part of the temporalis muscle. The passive and active length-tension characteristics of muscle suggest that the CR should be located in the region of the insertions of these muscles in most mammals[2] (Carlson, 1977; Hylander, 1992; Weijs et al., 1989). Specifically, the passive tension in these muscles is an important determinant of the location of the CR that acts to put the CR near the insertions of these muscles during jaw opening (Weijs et al., 1989). The need to keep these muscle fibers within an effective range of their length-tension curves during the power stroke also constrains the location of the CR to be near the insertion sites of these muscles and therefore some distance from the condyle (Carlson, 1977; Hylander, 1992).

It is predicted that pure mandibular translation will be relatively rare during mastication and that, as a result, angular rotation about a transverse axis will be highly correlated with the amount of sagittal condylar sliding during mastication (cf. Hylander et al., 1987). It is also predicted that pure angular rotation of the condyle about a transverse axis will be rare. If true, this will indicate that the CR is rarely located at the condyle. Finally, it is predicted that interspecific differences in sagittal sliding will be correlated with variation in the location of the CR such that the larger the distance between the CR and the condyle, the more sagittal sliding will occur for a given angular rotation (Fig. 3).

Two questions are evaluated in a sample of nonhuman anthropoid primates in an attempt to test these predictions and refine that portion of the hypothesis concerning the functional relation of TMJ design to condylar movement. These questions are 1) what the extent of sagittal condylar sliding during mastication is and 2) how interspecific differences in sagittal condylar sliding are related to other kinematic parameters (such as linear gape) and to structural features (such as jaw size and the shape of the joint surfaces).

The cineradiographic data include films of *Ateles* spp., *Macaca fascicularis, Papio anubis,* and *Pan troglodytes.* So the hypothesis that sagittal condylar sliding is functionally related to TMJ shape could be tested, measurements of the mandible and the TMJ of *A. geoffroyi, M. fascicularis, P. anubis,* and *P. troglodytes* were analyzed. The morphometric results are presented first. Then the cineradiographic data are presented and evaluated with the morphometric data in order to answer the two questions about sagittal condylar sliding posed in the previous paragraph. The results of both analyses are used to develop the functional model. Predictions about the effects of two aspects of diet, the mechanical properties and the size of food objects, on condylar motion and TMJ shape derive from the model.

MATERIALS AND METHODS

Morphometry sample and data analysis

The mandible and the left TMJ of at least ten wild-caught individuals of *Ateles geoffroyi, Macaca fascicularis, Papio anubis,* and *Pan troglodytes* were measured (Table 1). Adult individuals with relatively unworn molar teeth were measured in order to control for ontogenetic influences on joint morphology, particularly age-related remodeling of the bony articular surfaces (Ashton and Zuckerman, 1954; Lindblom, 1960; Mof-

[2]Bony structures, such as the postglenoid and preglenoid processes of some Carnivora, may constrain the location of the CR to the condyle. The high mobility of the condyle indicates that the primate TMJ lacks such bony constraints.

TABLE 1. Sample used in the morphometric study of mandibular and joint dimensions[1]

Species	Sample size F	M	Age	Average weight (kg)	
Ateles geoffroyi	5	5	Adult	7.3 (F)	7.8 (M)
Macaca fascicularis	5	5	Adult	3.6 (F)	5.4 (M)
Papio anubis	4	6	Adult	13.3 (F)	25.1 (M)
Pan troglodytes[2]	6	6	Adult	45.8 (F)	59.7 (M)

[1] All specimens were wild-caught. F, female; M, male. Average weight taken from Smith and Jungers (1997).
[2] *P. troglodytes troglodytes* was measured, and the average weights reported are for this subspecies.

TABLE 2. List of TMJ measurements defined in the text and their abbreviations

Relative depth of the articular eminence	RELAE
Anteroposterior curvature of the condyle	APCurve
Coronal curvature of the condyle	COCurve
Curvature of the medial half of the coronal aspect of the condyle	MCurve
Curvature of the lateral half of the coronal aspect of the condyle	LCurve
Length of the articular eminence	ArtLgth
Length of the glenoid fossa	GlenLgth
Shape of the entoglenoid process	EntShape
Angle of the articular eminence relative to the plane of the glenoid fossa	Slope

fett et al., 1964; Oberg et al., 1971; Granados, 1979; Hinton, 1981).

A list of the measurements and their abbreviations is in Table 2. The TMJ was molded in vinyl polysiloxane (Express; 3M Corp.), and epoxy casts were made from the molds. Mold shrinkage after 1 year was between 0.05% and 0.09% (for similar results see Teaford and Oyen, 1989). RELAE, APCurve, COCurve, MCurve, and LCurve were measured from traces of the casts. The traces were made using a microscope fitted with a camera lucida attachment. The traces were digitized using a digitizing tablet (Summagraphics) and software (SigmaScan; Jandel Corp., Corte Madera, CA) that calculated curvilinear and linear distances. ArtLgth, GlenLgth, and EntShape were measured on the casts with sliding digital calipers accurate to the nearest 0.1 mm. Slope was measured at 90° to the long axis of the cranium (inion to prosthion) from photographs of the articulated cranium and mandible of each specimen in lateral view. In order to minimize distortions due to parallax, the camera-to-object distance was between 3 and 8 feet.

Mandibular length is the distance in millimeters from the infradentale to the posterior border of the mandible taken parallel to the molar tooth row (Cole, 1992) (Fig. 4). The variable ascending ramus height in millimeters (Fig. 4) was used as a structural correlate of the distance between the condyle and the CR during mastication.

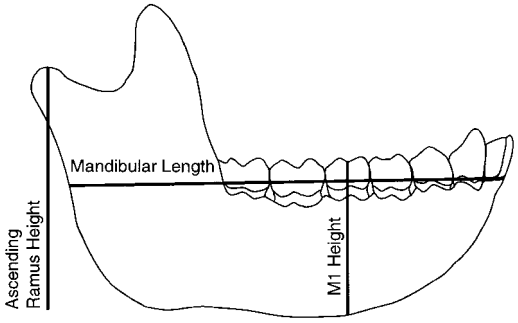

Fig. 4. Linear measurements taken on the mandible. See text for discussion.

The reference line for measuring the relative depth (the ratio RELAE) and the orientation (Slope in degrees) of the articular eminence was the line formed by the superior point on the glenoid fossa and the anterior margin of the preglenoid plane in lateral view (Fig. 5A). RELAE (Fig. 5A) is the depth of the articular eminence (d in Fig. 5A, the perpendicular distance from the reference line to the peak of the articular eminence) divided by the length of the articular eminence. For RELAE measurements, each cast was placed with its mediolateral axis oriented perpendicular to the microscope lens. The reference line was in the plane of the microscope lens. Slope (σ) was measured from the lateral photographs and is the angle subtended by the reference line and the line formed by the superior point on the glenoid fossa and the peak of the articular eminence (Fig. 5A). Slope could not be measured in *Ateles geoffroyi* because the zygomatic arch dips inferior to the peak of the articular eminence. The articular eminence is shallow in *A. geoffroyi*, and visual inspection shows that its slope is very acute compared to the other species in the sample. Slope in *A. geoffroyi* was given the rank of 1 in the rank order correlation analysis (see below).

The variable ArtLgth is the length of the articular eminence measured in millimeters

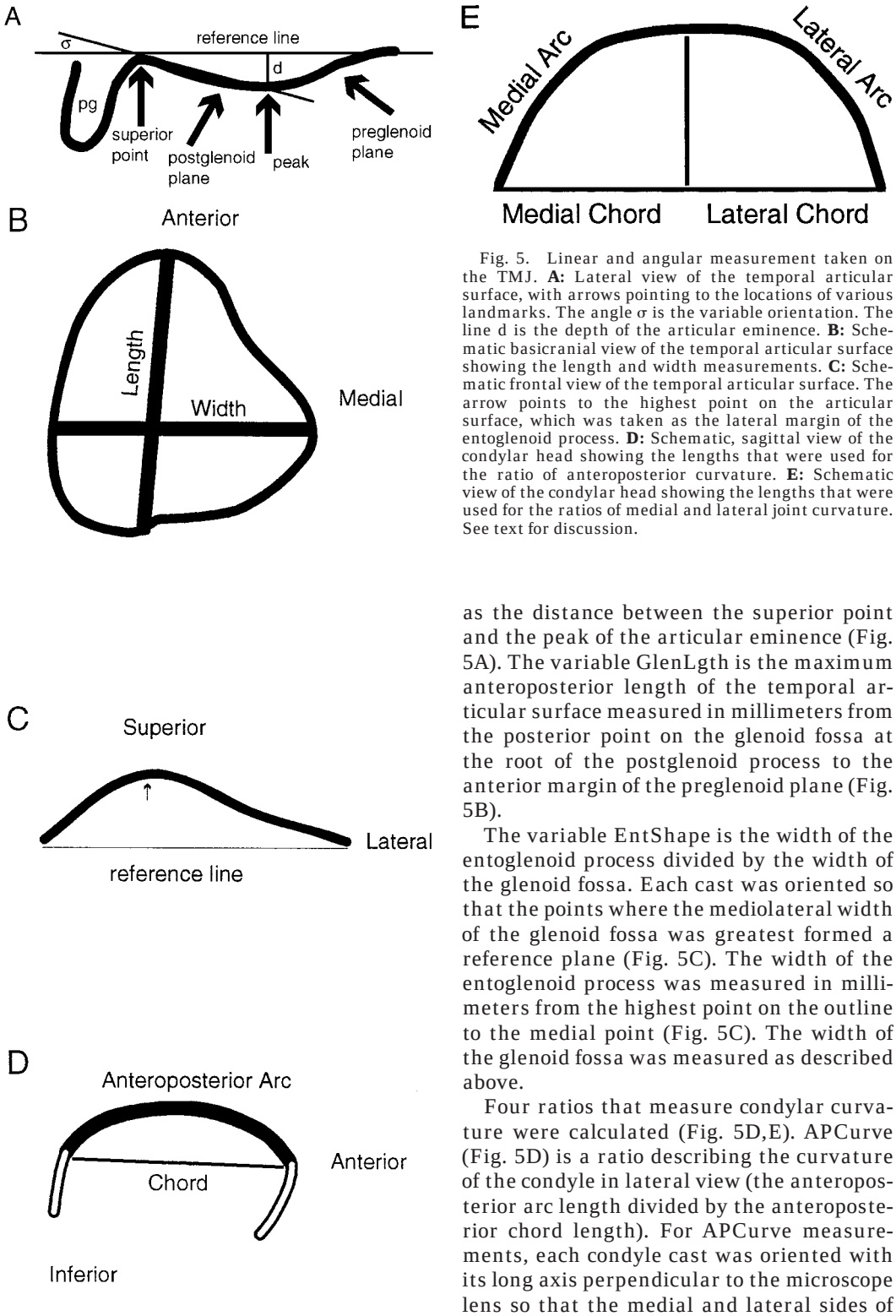

Fig. 5. Linear and angular measurement taken on the TMJ. **A:** Lateral view of the temporal articular surface, with arrows pointing to the locations of various landmarks. The angle σ is the variable orientation. The line d is the depth of the articular eminence. **B:** Schematic basicranial view of the temporal articular surface showing the length and width measurements. **C:** Schematic frontal view of the temporal articular surface. The arrow points to the highest point on the articular surface, which was taken as the lateral margin of the entoglenoid process. **D:** Schematic, sagittal view of the condylar head showing the lengths that were used for the ratio of anteroposterior curvature. **E:** Schematic view of the condylar head showing the lengths that were used for the ratios of medial and lateral joint curvature. See text for discussion.

as the distance between the superior point and the peak of the articular eminence (Fig. 5A). The variable GlenLgth is the maximum anteroposterior length of the temporal articular surface measured in millimeters from the posterior point on the glenoid fossa at the root of the postglenoid process to the anterior margin of the preglenoid plane (Fig. 5B).

The variable EntShape is the width of the entoglenoid process divided by the width of the glenoid fossa. Each cast was oriented so that the points where the mediolateral width of the glenoid fossa was greatest formed a reference plane (Fig. 5C). The width of the entoglenoid process was measured in millimeters from the highest point on the outline to the medial point (Fig. 5C). The width of the glenoid fossa was measured as described above.

Four ratios that measure condylar curvature were calculated (Fig. 5D,E). APCurve (Fig. 5D) is a ratio describing the curvature of the condyle in lateral view (the anteroposterior arc length divided by the anteroposterior chord length). For APCurve measurements, each condyle cast was oriented with its long axis perpendicular to the microscope lens so that the medial and lateral sides of

the superior-facing aspect of the articular surface were in alignment. From this perspective, the part of the condylar outline with the greatest curvature was digitized, and the chord formed between the most posterior and the most anterior point on the curve of this outline was digitized (Fig. 5D).

COCurve measures the curvature of the condyle in the plane of the medial and lateral poles of the condyle (Fig. 5E). This plane lies between the coronal and sagittal planes. MCurve measures the curvature of the medial half of the condyle in this plane (Fig. 5E). LCurve measures the curvature of the lateral half of the condyle in this plane (Fig. 5E). For COCurve, MCurve, and LCurve measurements, each condyle cast was oriented with the axis connecting the medial and lateral poles parallel to the microscope lens. From this perspective, the part of the outline with the greatest curvature was digitized, and the chord formed between the medial and lateral poles was digitized.

SAS, version 5, for the IBM mainframe computer (SAS Institute Inc., 1985) and SAS–pc, release 6.03 (SAS Institute Inc., 1988), were used to perform the statistical analyses. Each variable was examined first for differences between males and females with analysis of variance (Proc ANOVA) on the ranked variates (Proc RANK). Depending on sample size, differences among taxa were evaluated using either the a posteriori Tukey or the a posteriori GT2 test (Proc GLM) on the ranked variates. The variates were ranked to approximate a nonparametric statistical evaluation (Conover and Iman, 1981) since small sample sizes precluded tests for normal distribution and homoscedasticity.

Cineradiography

Sample and experiments. Cineradiography permitted direct observation and quantification of condylar movement in *Ateles* spp. (one adult female, one adult male), *Macaca fascicularis* (two adult females, one adult male), *Papio anubis* (one male; data collected at 5 and 6 years of age[3]), and *Pan troglodytes* (two females; data collected when chimpanzee A was 6 years old (M2/2 erupted but not in occlusion) and chimpanzee B was 5 years old [M1/1 erupted][4]).

TABLE 3. Experiments available for the quantitative and qualitative analyses

Subject	Number of experiments	Foods eaten during these experiments
Ateles		
Female	5	Apple with skin, monkey biscuit
Male	8	Banana, plum, hard cookie, bread
Macaca		
Female A	2	Apple with skin
Female B	1	Apple with skin
Male	2	Apple with skin, monkey biscuit
Papio		
Male	3	Apple and pear with skin, plum, orange slice
Pan		
Female A	7	Apple and pear with skin, banana, plum, orange slice, licorice
Female B	6	Apple and pear with skin, banana, plum

The number of experiments analyzed for each subject is listed in Table 3. Data were recorded in lateral view (Fig. 6) during mastication of a variety of food items, including pieces of apple with skin attached, pear with skin attached, monkey biscuit, banana, plum fruit, hard cookie, bread, orange slices, and licorice (Table 3). The majority of the data was recorded during chewing pieces of either an apple or pear with skin attached (Tables 3, 4). These two foods were assumed to have similar physical properties and were treated as a single food for analysis.

Radiopaque markers were embedded in or affixed to the teeth of the long-tailed macaques, the male spider monkey, and the female chimpanzees. In the long-tailed macaques, the radiopaque markers were amalgam fillings embedded in the buccal side of the crowns of the left maxillary and mandibular canines and second molars. Hylander et al. (1987) provide details of the attachment procedures for the these subjects. In the other subjects, the small (0.7 mm diameter), stainless steel ball was bonded to the buccal side of the tooth crown with a small

[3]The adult canines erupted over the time that the recordings were made.

[4]In both chimpanzees, the adult canines erupted slightly during the 3 month period during which they were filmed.

Fig. 6. Lateral view of part of the head and neck of the *Papio* male. This image was taken from a frame of the cineradiographic film. Digitizing landmarks on the maxillary and mandibular M1s and M2s are shown with a black-ringed, white circle. The erupting M_3 is labelled. The sharpness and contrast of this image are significantly reduced compared to the original 35 mm film because it was transferred from film to videotape and then from videotape to a digital computer file prior to printing.

TABLE 4. The digitized data sets[1]

Species, subject, data set	Food	Number of cycles	Number of frames	Chewing side
Ateles				
Female, 1	Apple	4	74	SI
Female, 2	Apple	16	152	SI
Macaca				
Female A, 1	Apple	5	149	BS
Female A, 2	Apple	10	409	WS
Female A, 3	Apple	16	583	WS
Female B, 1	Apple	7	348	WS
Male, 1	Apple	3	111	BS
Papio				
Male, 1	Apple/pear	4	35	SI
Male, 2	Apple/pear	3	33	SI
Male, 3	Apple/pear	1	16	SI
Pan				
Female B, 1	Apple/pear	4	95	SI
Female B, 2	Apple/pear	2	16	SI

[1] Apple, apple pieces with skin attached; Apple/pear, apple and pear pieces with skin attached; BS, balancing side; SI, side indeterminate; WS, working side.

amount of dental restorative resin (APH; L.D. Caulk Co.). For the male spider monkey, markers were present on the teeth, but no data were digitized for this study because he would not eat apple or pear with skin attached. For chimpanzee A, markers were present on the teeth, but no data were digitized for this study because there were either large out-of-plane head movements or loss of data when the canine marker dropped out of the image field. For chimpanzee B, the markers that were digitized were affixed to the right maxillary and mandibular canines and second deciduous molar.

The female spider monkey and the baboon did not have radiopaque markers on the teeth. The tip of the maxillary and mandibular incisor tooth row and the M3 distal cervix were digitized on the female spider monkey. The tip of the maxillary first molar trigon and second molar talon and the tip of the mandibular first molar trigonid and second molar talonid were digitized on the baboon (Fig. 6).

The 16 mm films of the long-tailed macaques were collected by W.L. Hylander and A.W. Crompton. Details of the recording

procedure and apparatus are provided in Hylander and Crompton (1980, 1986) and Hylander et al. (1987). The 16 mm films of the female spider monkey were collected by R.F. Kay and K.M. Hiiemae, and details of the recording procedure and apparatus are given in Kay and Hiiemae (1974a,b).

The films of the male spider monkey, the baboon, and the chimpanzees were collected by the author. The X-ray images were produced using a cineradiography apparatus (Philips Corp.) fitted with an X-ray source, an image intensifier, and a 35 mm cine camera. The X-ray image field was 9 inch by 9 inch square. Films were recorded at a rate of either 60 or 90 frames per second. The camera was shuttered so that each frame of the high resolution, 35 mm film (Varicath VCI 300U (Vari-X Corp.) or Cinerex CNP2, [AGFA-Gevaert Corp.]) was exposed by a 1 msec X-ray pulse. Subjects were seated in a plexiglass box that allowed free movement of the head and body during recording sessions. The chimpanzee subjects were trained to elevate their heads through a hole at the top of the box while seated comfortably. Subjects generally fed themselves. Occasionally, the female chimpanzee subjects were hand-fed using a 2-foot-long plastic pincer.

Data analysis. Areas of the TMJ seen radiographically in sagittal view were defined as follows. The articular eminence extends anteriorly from the superior point to the peak of the articular eminence (Fig. 5A). The preglenoid plane is the part of the articular surface extending anteriorly from the peak of the articular eminence to the anteriormost margin of the temporal articular surface (Fig. 5A). Its anterior margin cannot be identified in the X-ray films. Of course, it was not possible to identify the articular disc. Dissections show that the articular disc is tightly attached to the condyle and loosely attached to the temporal bone in all species (Rees, 1954; Schmolke, 1990; Wall, 1995).

For most of the analyses described below, the radiopaque markers or anatomical landmarks were digitized from sequences during which apple or pear with skin was chewed. Table 4 lists the number of chewing cycles and frames digitized for these data sets.

Skull movements in the plane of the camera were held constant by creating a reference plane with the maxillary markers (Hylander and Crompton, 1980, 1986; Hylander et al., 1987). The location of a point on the superior surface of the condyle was digitized in a pure lateral reference frame at the beginning of each chewing sequence. A pure lateral reference frame was identified visually as a frame in which all visible structures found on both the left and right sides of the head were perfectly superimposed (e.g., the left and right M^3). The coordinates of the point on the condyle were mathematically inserted into each subsequent frame of film by assuming that this point was a fixed distance and angle from the mandibular markers. This approach is based on the methods of Hylander et al. (1987), and the formulae to calculate the coordinates of the derived condylar point were derived by Mr. David Hertweck (Department of Biological Sciences, University of Cincinnati). X-axis condylar movement occurs along the axis defined by the maxillary markers. Y-axis movement occurs at a right angle to this axis.

Mathematical determination of the condylar point is sensitive to the magnitude of the out-of-plane rotation of the head. The error due to out-of-plane rotation was calculated using the method of Miller and Petak (1973). This error is nonlinear and is small up to about 17° of out-of-plane movement (Miller and Petak, 1973). Out-of-plane rotation averaged approximately 6° and was less than 10° in the majority of frames. Frames in which greater than 17° of out-of-plane movement occurred were not analyzed. Errors due to out-of-plane rotation and digitizing error were reduced by magnification of the film frames to between 1.5 and 2.9 times actual size.

A number of variables were quantified from the digitized sequences. Linear gape is the distance in pixels between the anterior digitizing landmarks (Fig. 7). FANG is the magnitude of the frame-to-frame angular rotation of the mandible about a transverse axis (α, Fig. 7). It is the angle in degrees through which the line passing between the derived condylar point and the posterior mandibular marker rotates in each frame. FANG is not the same as a measurement of

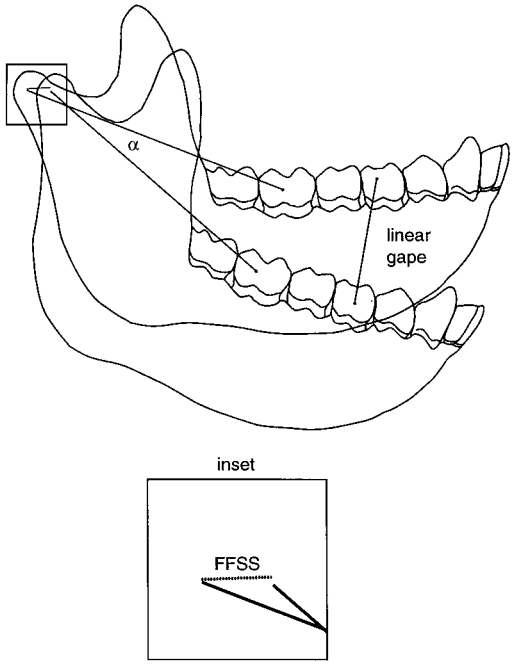

Fig. 7. The kinematic variables: frame-to-frame sagittal sliding (FFSS), frame-to-frame angular gape (α, or FANG in the text), and linear gape. All the cumulative variables are derived from FFSS and α (FANG). **Inset:** Enlarged view of boxed area.

frame-to-frame angular rotation about the mandibular CR. Angular gape is cumulative angular rotation of the mandible about a transverse axis.

In this analysis, linear gape and angular gape are distinguished from each other because variation in mandibular size, particularly mandibular length, influences interindividual comparisons of angular gape. A long-jawed animal can open its mouth to accommodate a 2 cm food item with much less angular gape than a short-jawed animal. In other words, linear gape is the same in both animals even though angular gape is very different. Gape also varies substantially during a single chewing sequence (Hylander et al., 1987). Two important factors that are positively correlated with gape are food size and food consistency, both of which change from cycle to cycle (Chew et al., 1988; Diaz-Tay et al., 1991; Postic et al., 1991). For these reasons, it was important to control for the influence of angular gape on sagittal condylar sliding. This is particularly important to this study because there was no way to control for food object size (the subjects were filmed by different researchers at different times).

The variables that measure sagittal sliding are frame-to-frame x-axis sliding in pixels (FFSS, Fig. 7), cumultive x-axis condylar sliding relative to the peak of the articular eminence (cumulative x-axis sliding in pixels/articular eminence length in pixels = RELX), and an estimate of absolute x-axis condylar sliding (RELX * mean articular eminence length in millimeters for the skeletal sample). For the digitized data, the x-axis movement of the condyle was much smoother than the y-axis movement because the y-axis movement was smaller and as a result more sensitive to the magnitude of the out-of-plane rotation. Although it would be preferable to include y-axis movement, analyses of the digitized data were confined to the x-axis sliding movement to minimize the computational error. For each subject, x-axis sliding was significantly correlated with y-axis sliding ($r = 0.571–0.986$, $P < 0.0001$).

The relative contributions of pure angular rotation and pure translation to the sagittal sliding movement of the condylar point were evaluated from the digitized data sets by comparing the frequency distributions of frames in which low, average, or high amounts of angular gape and sagittal sliding occurred. Two variables, rotation and slide, were created. If the value for FANG was within one standard deviation (s.d.) of the mean for that data set, rotation was designated as average for that frame. If the value for FFSS was within 1 s.d. of the mean for that data set, slide was designated as average for that frame. Values of FANG and FFSS greater than or less than 1 s.d. were designated as high or low frames for rotation and slide, respectively. Next, a new variable, Match, was created. When rotation and slide were both average, both high, or both low, Match was counted as yes. Mismatches were counted as highslide (1 s.d. more FFSS than FANG), veryhighslide (2 s.d. more FFSS than FANG), highrot (1 s.d. more FANG than FFSS), and veryhighrot (2 s.d. more FANG than FFSS). For example, a frame was designated as veryhighslide if the FFSS value was high and the FANG value was

low. Large numbers of veryhighslide frames in the data sets indicate that mandibular translation is a large part of the sagittal sliding movement and will falsify the prediction that the amount of sagittal sliding is primarily a function of angular gape.

Spearman's and Kendall's rank-order correlations between absolute condylar sliding (ABX) and ascending ramus height in the skeletal sample were computed in order to test the prediction that the amount of sagittal sliding is correlated with the distance between the CR and the condyle.

For the standardization of absolute sagittal sliding to joint size, sagittal sliding relative to the peak of the articular eminence (RELX) was used to explore the relation between TMJ shape and sliding. Three analyses were designed to capture information about relative sagittal sliding of the condyle. Relative sagittal sliding was measured as a discrete variable at the maximum angular gape for each chewing cycle during chewing of all foods (no angular gape or food consistency controls). This analysis has several advantages. It includes data for the male spider monkey and female chimpanzee A (compare Tables 3 and 4), it includes information on y-axis condylar sliding, and large numbers of chewing cycles for each subject were available because precise head movements did not restrict analysis. The relative amount of sagittal sliding in each chewing cycle was assessed for each subject at maximum angular gape by counting each time that the midpoint of the condyle remained posterior to the peak of the articular eminence (scored -1), reached the peak of the articular eminence (scored 0), or moved anteriorly onto the preglenoid plane (scored +1). Mean values close to +1 indicate substantial forward sliding of the condyle relative to the articular eminence during the opening stroke, whereas mean values close to -1 indicate relatively small amounts of sliding. G-tests (Sokal and Rohlf, 1981) determined whether significant between-individuals and between-species differences in the condylar movement counts were present.

In the second analysis, RELX measured at the maximum angular gape for each chewing cycle during chewing of a standard food was analyzed (food consistency control). For the third analysis, RELX measured at a constant angular gape (the covariate in an unbalanced ANCOVA) during chewing of a standard food was analyzed (angular gape and food consistency control).

The statistical analyses were carried out using SAS-pc, release 6.03 (SAS Institute, Inc., 1988). Angular gape, FFSS, FANG, and RELX were tested for normality using the Shapiro-Wilk (W) statistic using Proc UNIVARIATE. These variables were normally distributed, and parametric tests were used. Nested analysis of covariance (ANCOVA) was performed using Proc GLM for unbalanced data. Rather than testing for homogeneity of slopes and equality of intercept, this method calculates the least-squares mean of the dependent variable (the adjusted Y value) adjusted for the mean value of the independent variable (the covariate).

Correlations between sagittal sliding relative to the peak of the articular eminence at a standard angular gape (the least-squares mean value for RELX from the ANCOVA analysis) with the variables describing TMJ structure were evaluated qualitatively. Spearman's and Kendall's rank-order correlations coefficients were also computed (Proc CORR). With a sample size of four taxa, statistical significance could be demonstrated only for a correlation of ± 1.0.

RESULTS

Morphometrics of the jaws and TMJ

The descriptive statistics for mandibular length and ascending ramus height are provided in Table 5. The sample can be divided into a small-sized and short-jawed group (*Ateles* and *Macaca*) and a large-sized, long-jawed group (*Papio* and *Pan*). Because of their long mandibles, *Papio* and *Pan* can achieve a large linear gape with a small angular gape compared to *Ateles* and *Macaca*. This underscores the importance of standardizing angular gape in comparisons of sagittal condylar sliding.

The mean values for ascending ramus height vary substantially in this sample (Table 5). *Macaca* has the shortest ascending ramus, followed sequentially by *Ateles*, *Papio*, and finally *Pan*. The prediction is that the absolute amount of sagittal condylar sliding per unit of angular gape should

TABLE 5. Variables describing mandibular size and TMJ size and shape[1]

	Mandibular length[2]			Ascending ramus height[3]			RELAE (mm/mm)[5]			Slope (°)[6]			APCurve (mm/mm)[7]			ArtLgth (mm)[8]			GlenLgth (mm)[9]			EntShape (mm/mm)[10]			COCurve (mm/mm)[11]			MCurve (mm/mm)[12]			LCurve (mm/mm)[13]		
	Mean	s.d.	N	Mean	s.d.	N	Mean	s.d.	N	Mean	s.d.	N	Mean	s.d.	N	Mean	s.d.	N	Mean	s.d.	N	Mean	s.d.	N	Mean	s.d.	N	Mean	s.d.	N	Mean	s.d.	N
Ateles geoffroyi																																	
Males	64.9	3.8	5	40.5	2.9	5	0.28	0.04	5	NA			1.21	0.08	5	5.0	0.4	5	12.6	0.8	5	0.29	0.04	5	1.13	0.02	5	1.18	0.03	5	1.07	0.02	5
Females	64.4	3.0	5	41.0	3.1	5	0.20	0.07	5	NA			1.24	0.05	5	6.1	0.6	5	13.1	1.8	5	0.27	0.03	5	1.17	0.03	5	1.23	0.04	5	1.09	0.03	5
Macaca fascicularis																																	
Males	75.8[14]	5.6	5	31.5	1.5	5	0.29	0.05	5	20.0	5.5	5	1.26	0.02	5	6.3	1.3	5	15.4	1.5	5	0.20[14]	0.02	5	1.09	0.02	5	1.11	0.02	5	1.07	0.02	5
Females	65.9	2.4	5	30.5	3.9	5	0.31	0.06	5	24.6	4.9	5	1.29	0.08	5	6.0	0.7	5	13.5	1.6	5	0.24	0.02	5	1.10	0.05	5	1.12	0.06	5	1.09	0.04	5
Papio anubis																																	
Males	139.3[4]	9.0	6	51.6	5.5	6	0.33	0.10	6	31.5	1.3	4	1.30	0.05	6	11.8	1.5	6	23.0	1.4	6	0.21	0.04	6	1.07	0.03	6	1.07	0.04	6	1.07	0.03	6
Females	122.4	16.8	4	50.6	11.4	4	0.29	0.13	4	31.3	1.5	3	1.30	0.09	4	9.2	0.6	4	20.8	2.0	4	0.22	0.06	4	1.08	0.02	4	1.10	0.04	4	1.07	0.01	4
Pan troglodytes																																	
Males	133.5	5.3	6	63.8	7.1	6	0.41	0.11	6	22.4	4.0	5	1.16	0.03	6	11.8	1.1	6	24.7	1.4	6	0.28	0.01	6	1.13	0.06	6	1.18	0.09	6	1.09	0.03	6
Females	127.7	4.6	6	54.2	8.9	6	0.46	0.05	6	23.3	5.8	6	1.19	0.06	6	11.7	0.9	6	23.3	2.4	6	0.28	0.03	6	1.10	0.03	6	1.12	0.05	6	1.07	0.03	6

[1] NA, not available (see text for discussion).
[2] The GT2 tests showed that *Ateles* and *Macaca* had significantly shorter mandibles than *Papio* or the *Pan* males and females and that *Ateles* had significantly shorter mandibles than the *Macaca* males.
[3] The Tukey tests showed that *Ateles* had a significantly shorter ascending ramus than *Papio* or *Pan* and that *Macaca* had a significantly shorter ascending ramus than *Ateles*, *Papio*, or *Pan*.
[4] The *Papio* male-female comparison approached significance for mandibular length.
[5] The Tukey tests showed that *Pan* has significantly higher value than *Ateles*, *Macaca*, or *Papio*.
[6] For some specimens of *Macaca, Papio,* and *Pan,* the articular eminence could not be distinguished accurately enough in the photographs to derive Slope. The Tukey tests showed that *Papio* has a significantly higher value than *Macaca* or *Pan*.
[7] The Tukey tests showed that *Macaca* has a significantly higher value than *Pan* and that *Papio* has a significantly higher value than *Ateles* or *Pan*.
[8] The Tukey tests showed that *Ateles* and *Macaca* have significantly smaller values than either *Papio* or *Pan*.
[9] The Tukey tests showed that *Ateles* and *Macaca* have significantly smaller values than either *Papio* or *Pan*.
[10] The Tukey tests showed that *Ateles* and *Pan* have significantly larger values than *Macaca* males or *Papio*.
[11] The Tukey tests showed that *Ateles* has a significantly higher value than *Macaca* or *Papio* and that *Pan* has a significantly higher value than *Papio*.
[12] The Tukey tests showed that *Ateles* and *Pan* have significantly higher values than *Papio* and that *Ateles* has a significantly higher value than *Macaca*.
[13] The ANOVA was not significant ($F = 0.75$, $P < 0.531$).
[14] Significant difference between sexes within a species.

be positively correlated with ascending ramus height. Therefore, sagittal condylar sliding should also increase in the same order as ascending ramus height.

There are two variables that measure absolute joint size. ArtLgth is similar in *Ateles* and *Macaca* and also in *Papio* compared to *Pan* (Table 5). There is more interspecific variability in GlenLgth, but *Ateles* and *Macaca* have a short temporal articular surface in comparison to *Papio* and *Pan* (Table 5).

The descriptive statistics for the ratios that describe the shape of the TMJ are provided in Table 5. An examination of RELAE shows that the sample can be divided on the basis of the relative depth of the articular eminence into a group with a relatively shallow articular eminence (*Ateles*, *Macaca*, and *Papio*) and *Pan*. Compared to the other species, *Papio* has a vertically oriented articular eminence. *Pan* and *Macaca* have articular eminences of intermediate orientation. As described previously, *Ateles* has a relatively flat articular eminence.

An examination of APCurve shows that there is a group with a condyle that is anteroposteriorly flat (*Ateles* and *Pan*) and a group with a condyle that is anteroposteriorly curved (*Macaca* and *Papio*). An examination of EntShape shows that *Ateles* and *Pan* have a relatively wide entoglenoid process compared to *Macaca* and *Papio* (Table 5). This is also reflected in the higher values for COCurve and particularly for MCurve in *Ateles* and *Pan* (Table 5). Lateral curvature (LCurve) of the condyle in this plane is nearly identical in all four species (Table 5).

General patterns of condylar movement

In all of the subjects, the mandible rotated about a transverse axis during mastication, and the condyle slid and rolled forward (during jaw opening) or backward (during jaw closing). The preglenoid plane was also an important movement surface during mastication, and it was used by all of the subjects during the wide gapes associated with incision and wide opening.

As predicted based on the results of Hylander et al. (1987), during mastication the amount of sagittal condylar sliding on the articular eminence and the preglenoid plane for an individual subject was variable and strongly positively correlated with linear gape and with angular gape (Table 6).

TABLE 6. Pearson product-moment correlation coefficients (r) of RELX with linear gape (in pixels to include the subjects without dental markers) and angular gape (°)[1]

	RELX with linear gape	RELX with angular gape
Ateles		
r	0.63	0.65
N	226	225
Macaca		
r	0.90	0.91
N	1,600	1,681
Papio		
r	0.63	0.66
N	84	84
Pan		
r	0.71	0.76
N	106	105

[1] Computed for *Ateles* sp. (one subject), *Macaca* (three subjects), *Papio* (one subject), and *Pan* (one subject) during apple/pear with skin mastication. N, number of frames.
* $P < 0.0001$ for all correlations.

TABLE 7. Percentage of frames in which average, high, and low amounts of frame-to-frame sagittal sliding (FFSS) and frame-to-frame angular gape (FANG) occurred in Ateles, Macaca, Papio, and Pan during mastication of apple/pear with skin[1]

Variable	*Ateles*	*Macaca*	*Papio*	*Pan*
FFSS				
Average	72.7	75.2	70.3	87.3
High	15.5	13.9	14.1	9.5
Low	11.8	10.9	15.6	3.2
FANG				
Average	78.1	72.4	68.7	80.0
Low	10.7	12.6	12.5	11.6
High	11.2	15.0	18.8	8.4

[1] See Table 3 for the number of individuals, chewing cycles, and film frames in the sample.

Integration of angular gape and sliding during mastication

Both frame-to-frame angular rotation (FANG) and frame-to-frame sagittal sliding (FFSS) were within 1 s.d. of the mean in 69–87% of all frames. The percentage of film frames in which FFSS was greater than 1 s.d. above average ranged from about 9% to about 16% (Table 7). The percentage of frames in which FANG was greater than 1 s.d. above average ranged from about 8% to about 19% (Table 7).

The frequency distributions of the variable Match showed that the amounts of FFSS and FANG relative to one another

TABLE 8. Percentage of film frames in which frame-to-frame sagittal sliding (FFSS) and frame-to-frame angular gape (FANG) occurred in similar relative magnitudes in Ateles, Macaca, Papio, *and* Pan *during apple/pear with skin mastication*[1]

Match	*Ateles*	*Macaca*	*Papio*	*Pan*
Yes	66.0	66.0	53.0	76.0
Highrot	15.0	14.0	23.0	10.0
Veryhighrot	0.5	0.5	0.0	0.0
Highslide	17.0	18.8	22.5	14.0
Veryhighslide	1.5	0.7	1.5	0.0

[1] See Table 3 for the number of individuals, chewing cycles, and film frames in the sample. The among-species G-test was not significant. See text for discussion.

TABLE 9. Condylar position relative to the peak of the articular eminence (counts) in each subject during mastication of the foods listed in Table 2[1]

Species, individual	Counts				
	−1	0	+1	N	Mean
Ateles spp.					
Female	19	52	6	77	−0.17
Male	4	34	12	50	+0.21
Macaca fascicularis					
Female A	0	39	15	54	+0.31
Female B	0	37	17	54	+0.28
Male[2]	0	2	1	3	+0.33
Papio anubis					
Male	18	7	0	25	−0.72
Pan troglodytes					
Female A	0	8	27	35	+0.77
Female B	0	4	12	16	+0.75

[1] Abbreviations: −1, condyle posterior to peak of articular eminence; 0, condyle at peak of articular eminence; +1, condyle anterior to peak of articular eminence; N, number of chewing cycles.
[2] Although many chewing cycles were available for quantitative analysis of dental movements and the derived condylar point in this subject, only three chewing cycles included film frames that had the condyle in view at maximum angular gape.

were similar across species (Table 8). Furthermore, in each species, frames with slightly high sagittal sliding relative to angular rotation or slightly high angular rotation relative to sagittal sliding occurred with nearly equal frequency. A predominance of sagittal sliding relative to angular rotation was quite rare for each species (veryhighslide ranged from 0–1.5 % of film frames) (Table 8). In addition, a predominance of angular rotation relative to sagittal sliding was even rarer (veryhighrot ranged from 0–0.5%). The G-test was not significant. The variable Match was also compared across species over various intervals during chewing (maxillary and mandibular teeth in contact, opening stroke, closing stroke). These G-tests were not significant.

Absolute and relative condylar sliding during mastication

Analyses of absolute and relative sagittal sliding of the condyle are presented in Tables 9–12. The analysis of relative sagittal sliding presented in Table 9 is the most complete in that the number of chewing cycles for each species is large and the y-axis sliding of the condyle is incorporated. No subject showed a bimodal distribution of the range of condylar movement counts where individual values were either -1 or +1. As a result, the mean values reflect the most commonly observed position of the condyle relative to the peak of the articular eminence.

An among-individuals G-test was performed. The results showed that the male and female spider monkeys were significantly different from one another ($G = 110.68$, $P < 0.001$). More movement relative to the peak of the articular eminence in the male spider monkey may be due in part to the larger size of the banana pieces and the harder consistency of the cookie pieces eaten by the male in comparison to the apple pieces eaten by the female (Table 2).

An among-groups G-test was performed. The sample was divided into five groups: female spider monkey, male spider monkey, long-tailed macaques, male baboon, and chimpanzees. The results were highly significant ($G = 159.83$, $P < 0.001$). Interestingly, this test showed no significant differences between the male and female spider monkeys. This indicates that, when the entire sample was analyzed, the distribution of the range of movement counts in the male and female *Ateles* subjects was more similar to one another than either was to another species.

The species mean values for *Pan* were very high (+0.76, N = 51), whereas those for *Macaca* (+0.30, N = 111) and *Ateles* (-0.04, N = 127 chewing cycles) were closer to zero. The mean value for the *Papio* subject (-0.72, N = 25 chewing cycles) approached -1.0.

As expected, maximum angular gape during apple or pear with skin mastication varied substantially both within and among species (Table 10). Both of the long-jawed subjects (*Papio* and *Pan* female A) had mean

TABLE 10. Relative sagittal condylar sliding (RELX) and angular gape at maximum gape during apple/pear with skin mastication[1]

Species, variable	Number of subjects	Number of chewing cycles	Mean	s.d.
Ateles	1			
Angular gape		20	13.8°	4.4°
RELX		19	0.71	0.2
Macaca	3			
Angular gape		39	15.7°	5.1°
RELX		38	0.79	0.3
Papio	1			
Angular gape		11	20.3°	4.3°
RELX		8	0.57	0.3
Pan	1			
Angular gape		7	21.8°	4.0°
RELX		5	1.17	0.3

[1] See Table 4 for number of film frames in the sample.

angular gapes of about 20°, whereas the short-jawed subjects (*Ateles* female and *Macaca*) had mean angular gapes of between approximately 14 and 16°. Linear gape was on average much greater in *Papio* and *Pan* than it was in *Ateles* or *Macaca* because of these high average angular gapes and because their mandibles are much longer (Table 5).

The results of the analysis of relative sagittal sliding at maximum angular gape during chewing of apple or pear with skin are given in Table 10. This analysis does not include information on y-axis motion. The condyle of the *Papio* subject had the least amount of relative sagittal sliding (RELX mean = 0.57). Larger amounts of relative sagittal sliding were observed in the *Ateles* female (RELX mean = 0.71), the *Macaca* subjects (RELX mean = 0.79), and in *Pan* female A (RELX mean = 1.17). The GT2 test showed that RELX in *Pan* female A was significantly higher than in the other subjects. There were no other statistically significant differences among subjects.

The comparison of relative sagittal sliding at a standard angular gape during chewing of apple or pear with skin showed that all of the species' least-squares means were significantly different from each other ($P < 0.0001$) (Table 11).

The estimates of absolute condylar sliding are given in Table 12 along with information about the rank order of absolute condylar sliding and ascending ramus height. The rank-order correlation between absolute condylar sliding and ascending ramus height is +1.0.

TABLE 11. ANCOVA results for relative sagittal condylar sliding (RELX) at a constant angular gape during apple/pear with skin mastication ($F = 82.33$, $P < 0.0001$)[1]

Species	Least-square mean RELX	Standard error	*P* least-square mean = 0
Ateles	0.43	0.01	0.0001
Macaca[2]	0.33	0.01	0.0001
Papio	0.26	0.02	0.0001
Pan	0.53	0.01	0.0001

[1] See Table 4 for number of individuals, chewing cycles, and film frames in the sample. The species least-squares means were all significantly different from each other at $P < 0.0001$.
[2] Least-square mean values for individuals are between 0.30 and 0.36. All *Macaca* individuals are significantly different from the other species ($P < 0.03$ and 0.0001 for *Papio* and $P < 0.0001$ for *Ateles* and *Pan*).

TABLE 12. Species means for articular eminence length, the estimate and rank order of the estimate of absolute sagittal sliding at a standard angular gape, and the rank order of the species means for ascending ramus height[1]

Species	Articular eminance length (mm)			Absolute sagittal sliding estimate		Ascending ramus height rank
	Mean	s.d.	N	(mm)	Rank	
Ateles spp.	5.6	0.8	10	2.4	2	2
Macaca fascicularis	6.2	1.0	10	2.0	1	1
Papio anubis	10.7	1.8	11	2.8	3	3
Pan troglodytes	11.8	1.0	12	6.2	4	4

[1] Absolute condylar sliding is estimated as (RELX at a constant angular gape) * (species mean articular eminence length in mm). See Table 11 for data on RELX at a constant angular gape and Table 5 for the means of ascending ramus height. The rank-order correlation coefficients between absolute sagittal sliding and ascending ramus height are $\sigma = +1.0$ ($P < 0.001$) and $\tau = +1.0$, ($P < 0.04$).

Correlations between sagittal sliding and joint shape

RELX (Table 11) is not correlated with either RELAE, Slope, or LCurve. RELX is negatively correlated with APCurve, and Kendall's ($P < 0.04$) and Spearman's ($P < 0.01$) correlation coefficients are −1.0 (Table 13). *Macaca* and *Papio* have curved condyles and low amounts of sagittal sliding relative to the peak of the articular eminence. *Ateles* and *Pan* show the opposite pattern. RELX has a strong relation to EntShape and to MCurve, although the correlations are not significant (Table 13). *Ateles* and *Pan* have relatively large entoglenoid processes and a curved medial aspect to the condyle in conjunction with high amounts of sagittal sliding relative to the peak of the articular

TABLE 13. Rank order of RELX and the TMJ shape variables with significant correlations highlighted

	Ranks					
Species	RELX	RELAE	Orient-ation	Ent-Shape	MCurve	AP-Curve
Ateles	3	1	1	4[2]	4	2
Macaca	2	2	2[1]	2	2	3
Papio	1	3	4	1	1	4
Pan	4	4	3[1]	3[2]	3	1

[1] The species mean values for orientation are essentially identical for *Macaca* (22.55°) and *Pan* (22.92°).
[2] The species mean values for EntShape are essentially identical for *Ateles* (0.281) and *Pan* (0.278).

eminence. *Macaca* and *Papio* show the opposite pattern.

DISCUSSION

These results provide new information about how the condyle moves during mastication and about how these movements are related to kinematic parameters and to structural features of the masticatory apparatus. As predicted, sagittal condylar sliding is highly correlated with angular rotation about a transverse axis (i.e., angular gape). Furthermore, pure mandibular translation was a very unusual movement during chewing. Also as predicted, pure angular rotation during mastication is rare, which indicates that the CR is rarely located at the condyle. These findings indicate that angular rotation about a transverse axis and mandibular translation are integrated during chewing. The condylar movements, sliding and rolling, that accompany these mandibular movements are also integrated. The frequency of frames in which relatively large amounts of angular rotation or sagittal sliding occurred (Table 7) indicates intraindividual and intraspecific variability in the location of the CR during chewing.

The prediction that the amount of sagittal condylar sliding is correlated with the distance between the CR and the condyle was evaluated by estimating absolute sagittal sliding in each species and calculating its correlation with ascending ramus height. As predicted, absolute sagittal sliding is highly positively correlated with ascending ramus height (Table 12) and by inference with the distance between the CR and the condyle. This result also suggests that ascending ramus height can be used to make inferences about the amount of absolute sagittal sliding in one species compared to another.

Gape was standardized for interspecific comparisons of relative sagittal sliding (Table 11) and in the correlations between relative sagittal sliding and the variables that describe TMJ shape. This meant that only a small number of chewing cycles could be analyzed for *Ateles*, *Papio*, and *Pan*. However, a comparison of the results for relative sagittal sliding at maximum angular gape demonstrates that the small data set (Table 10) is representative of the larger data set which includes y-axis sagittal sliding and large numbers of chewing cycles for each individual as well as data on the male spider monkey and a second female chimpanzee (Table 9).

The size and shape of the articular eminence and the temporomandibular ligament are thought to have an important role in keeping the condyle close to the articular eminence in humans (Rees, 1954; Osborn, 1989). Rees (1954) suggests that the depth and the vertical orientation of the human articular eminence cause tension to develop in the temporomandibular ligament during jaw opening. This tension helps to keep the condyle pressed against the articular eminence. Osborn (1989) suggests that this prevents erratic motion of the condyle against the articular eminence, particularly at the initiation of the closing stroke. Thus, in an interspecific comparison, we expect articular eminence depth or orientation to be positively correlated with sagittal sliding relative to the peak of the articular eminence. However, there was no correlation between the depth or the orientation of the articular eminence and relative sagittal sliding.

The absence of a correlation may be due to a lack of specificity between the shape of the articular eminence and this function. Vertical and horizontal fibers of the temporomandibular ligament lengthen during forward condylar motion regardless of the depth of the articular eminence (Fig. 8). A deep and steep articular eminence causes the temporomandibular ligament only to lengthen more than it would if the articular eminence was shallow and flat.

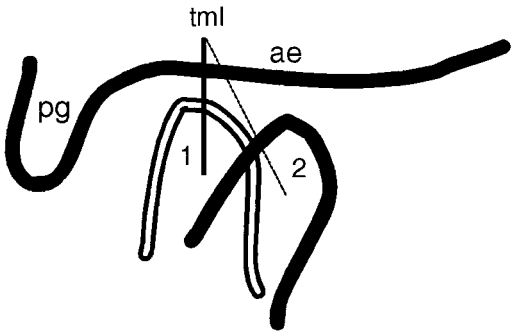

Fig. 8. Schematic, lateral view of the TMJ. The vertical fibers of the temporomandibular ligament lengthen during jaw opening (e.g., the condyle moves from position 1 to position 2) when the articular eminence is shallow and flat. ae, articular eminence; pg, postglenoid process; tml, temporomandibular ligament.

At least two other functions have been proposed for the articular eminence. Nickel et al. (1988a,b) suggested that in humans the articular eminence forms as a direct result of joint loading during feeding. However, experimental evidence and biomechanical theory suggest that a TMJ reaction force is present in all mammals during mastication and incision (e.g., Crompton, 1963; Hylander, 1975, 1979a; Greaves, 1978; Smith, 1978; Crompton and Hylander, 1986; Boyd et al., 1990). A hypothesis invoking joint loads does not explain the absence of an articular eminence in many mammals.

It has also been suggested that an articular eminence located laterally in the joint, as it is in extant monkeys and apes, increases the inferior and lateral movement of the balancing-side condyle during unilateral mastication (Humphreys, 1932; Angel, 1948; Mills, 1955, 1963, 1978; Moore, 1981; Mack, 1984). This ensures that the maxillary and mandibular teeth on the balancing side do not interfere with each other during the power stroke and obstruct the transverse shearing/grinding motion of the working-side teeth. More work needs to be done to describe interspecific variation in the size and shape of the articular eminence and the elastic properties of the temporomandibular ligament before these hypotheses can be evaluated.

Ateles geoffroyi, Macaca fascicularis, Papio anubis, and *Pan troglodytes* have nearly identical mean values for lateral condylar curvature (LCurve) (Table 5). The lateral part of the condyle articulates with the articular eminence during the power stroke. Flatness in this dimension increases joint contact area in the lateral part of the TMJ. Bone strain data indicate that the lateral part of the joint is more heavily loaded than the medial part (Hylander, 1979a). The similarity in values for lateral condylar curvature suggests that the shape of the lateral part of the condyle may be strongly constrained by the loading environment during the power stroke.

The functional model

The following functional explanations of the correlations between joint shape and relative sagittal sliding consider TMJ forces and movements during the power stroke. At large gapes during chewing and biting, compared to *Papio* and *Macaca, Ateles* and *Pan* have relatively more posterior condylar sliding. Substantial sliding occurs, for example, in the initial stages of chewing large pieces of food between the molars or during biting into large food objects between the incisors. Presumably large joint reaction forces occur simultaneously with relatively large amounts of posterior condylar sliding.

The combination of high forces and large amounts of sagittal sliding during the power stroke suggests that *Ateles* and *Pan* should have articular structures that help guide the path of the condyle. Erratic condylar movement during the power stroke could cause an unpredictable loading situation at the joint surfaces. A stabilizing structure is one that helps to decrease or prevent any tendency for the condyle to move in an undesired direction. Both *Ateles* and *Pan* have a relatively wide entoglenoid process that is highly congruent with the medial aspect of the condyle. Both of these structures are covered with articular tissue, which suggests that they contact one another. If the entoglenoid process contacts the medial condyle during the power stroke, the morphology seen in *Ateles* and *Pan* may help the entoglenoid process to act as a guide to sagittal sliding and may help to prevent excessive mediolateral condylar sliding.

The flattening of the anteroposterior curvature of the condyle (APCurve) seen in *Ateles* and *Pan* increases joint contact area, which lowers stresses. Also, a flat condyle creates a more congruent articulation with the articular eminence. Increased congruence may smooth the sagittal sliding and rolling motion of the condyle relative to the articular eminence and help to maintain integrated motion.

If a flat condyle reduces joint stress and helps to smooth the sliding and rolling motion of the condyle, then all primates should have flat condyles. Perhaps the benefits of flatness must be combined with the need for a rotatory joint surface, particularly during display behaviors when the jaws are opened extremely wide. The interplay of these influences may explain why we observe a range of anteroposterior condylar curvature.

Predictions of the functional model. The way in which TMJ shape will vary in association with the consistency and the size of food objects can be predicted from the functional model. The foundation of the following predictions is that ascending ramus height will be strongly and positively correlated with sagittal condylar sliding. The effect of ascending ramus height on relative sagittal sliding, an important variable for predicting entoglenoid process shape and anteroposterior condylar curvature, depends on the absolute length of the temporal articular surface. For example, although *Ateles* has absolutely small amounts of sagittal sliding (Table 12), relative sagittal sliding is large compared to the other species sampled here because *Ateles* has a short temporal articular surface (Tables 5, 11). Mandibular size may affect the magnitude of mandibular rotation since it influences linear gape per unit of angular gape and must be accounted for in predictions about correlations between TMJ shape and diet.

Mastication of resistant objects vs. soft objects. Resistant objects are defined as foods that require high occlusal loads (e.g., seeds) or large numbers of chewing cycles at moderate to high occlusal loads (e.g., leaves) to cause a reduction in particle size. In comparison to soft-object feeders, resistant-object feeders must generate absolutely higher bite forces and resist relatively high bending moments acting on the mandible. Although bite forces during folivory may not always be high compared to other food items, folivores must generate large numbers of power strokes during a single feeding bout (Hylander, 1979b).

These requirements suggest that, in order to increase muscle and bite force, resistant object feeders should increase the cross-sectional area of their jaw adductor muscles. An increase in the height of the ascending ramus increases the space available for the attachment of the masseter and medial pterygoid muscles (Freeman, 1988) and probably also the anterior temporalis muscle, thereby increasing their cross-sectional areas since these muscles have both tendinous and fleshy insertions. It has also been proposed that a tall ascending ramus lengthens the moment arms of the masseter and medial pterygoid muscles (Maynard Smith and Savage, 1959). An elevated condyle relative to the occlusal plane is often associated with a tall ascending ramus and is thought to enhance fore-aft and mediolateral grinding movements of the dentition (Lebedinsky (1938), as cited by Davis, 1964; Arendsen de Wolff-Exalto, 1951a,b; Greaves, 1980) and also to cause relatively uniform bite pressure along the tooth row (Arendsen de Wolff-Exalto, 1951a,b; Ward and Molnar, 1980).

The model predicts that resistant-object feeders will have absolutely large amounts of sagittal sliding due to a tall ascending ramus. The link between joint shape, food-object consistency, and relative sagittal sliding depends on the length of the temporal articular surface. When it is comparatively short, relative sagittal sliding will be high. The prediction is that large amounts of relative sagittal sliding will be correlated with a relatively wide, congruent entoglenoid process and an anteroposteriorly flat condyle.

Mandibular length may or may not be absolutely shorter in resistant-object feeders when compared to close relatives that feed on nonresistant food items. For example, folivores are often large-bodied (Kay, 1975) and would be expected to have abso-

lutely longer mandibles than smaller-bodied relatives.

Incision of large, resistant objects vs. small, nonresistant objects. Perhaps the biggest constraints operating during incision of large objects are related to gape. The jaws must be long enough to accommodate large objects between the teeth, and the muscles must be able to produce sufficient force at large gapes (cf. Herring and Herring, 1974). All else being equal, to achieve large gapes animals will have absolutely greater amounts of sagittal sliding when incising on large objects.

Species that incise large objects may be constrained (e.g., by the length of the temporal articular surface) to limit the increased absolute sagittal sliding associated with large gapes. One way to maintain or decrease sagittal condylar sliding to achieve a given linear gape is to increase mandibular length. Another way is to have a short ascending ramus. This maintains the relative position of the CR with respect to the adductor muscles and shortens its absolute distance from the condyle. These alternatives are not mutually exclusive.

Currently, the best data on food-size preference are for anthropoids that eat items that are both large and resistant (e.g., palm nut cracking in *Cebus apella*). The following predictions are made for species that incise relatively large and resistant objects as compared to similarly sized species that incise relatively soft and small objects.

During preparation of large and resistant food objects, high bite forces occur at large gapes. Therefore, species that incise large and resistant objects should not produce large gapes by increasing the length of the mandible. Instead, they should have absolutely short jaws. A short jaw reduces bending moments during incision (Hylander, 1979b) and may increase the efficiency of bite force production at the anterior dentition (Greaves, 1978).

During incision of large, resistant objects, high muscle forces are generated at large gapes. The height of the ascending ramus should increase for the reasons described earlier for resistant-object mastication. The effect of this is an increase in the distance between the CR and the condyle and increased sagittal condylar sliding. Relative sagittal sliding depends on the length of the temporal articular surface. The combined effects of a short mandible and a tall ascending ramus suggest that relative sagittal sliding will be very large in small-bodied species that incise large, resistant objects. High amounts of relative sagittal sliding will be associated with a relatively wide entoglenoid process, a medially curved condyle, and an anteroposteriorly flat condyle.

CONCLUSIONS

The hypothesis that the shape of the bony TMJ, the amount of sagittal sliding during chewing, and the mechanical properties and size of food objects are interrelated functionally was proposed. Two questions were investigated in an attempt to test and refine that portion of the hypothesis concerning the functional relation of TMJ design to condylar movement. The first question was to determine the extent of sagittal condylar sliding during mastication for each species. Both absolute and relative sagittal sliding exhibit high amounts of intraindividual variability during mastication. Much of this variability is linked to variation in angular gape. Interspecific contrasts must therefore be made by comparing absolute and relative sagittal sliding per unit of angular gape. When angular gape is standardized, absolute sagittal sliding is correlated with the height of the ascending ramus. Relative sagittal sliding depends on both absolute sagittal sliding and the length of the temporal articular surface.

The second question was to determine how interspecific differences in sagittal condylar sliding relate to other kinematic parameters and to structural features of the masticatory apparatus. Three predictions were supported: 1) pure mandibular translation is rare during mastication; 2) pure angular rotation is rare during mastication; and 3) the larger the distance between the CR and the condyle, the more sagittal sliding will occur for a given angular rotation. These results, along with the finding that sagittal sliding and angular rotation about a transverse axis are highly positively correlated with one another, indicate that sagit-

tal sliding and angular rotation are smoothly integrated during chewing.

There was no clear correlation between relative sagittal sliding and articular eminence shape. A number of hypotheses about the functional significance of the articular eminence have been proposed. More work needs to be done to describe variation in the size and shape of the articular eminence before these hypotheses can be evaluated. There was a strong negative correlation between the anteroposterior curvature of the condyle and relative sagittal sliding. In addition, there is a general though not statistically significant relation between the width of the entoglenoid process, the curvature of the medial part of the condyle, and relative sagittal sliding.

Predictions of the relation between food consistency and food-object size, TMJ shape, and mandibular shape rely on three connections. The first is that food consistency and food-object size affect the mechanical behavior of the masticatory apparatus and, with respect to influencing TMJ shape, interact significantly with ascending ramus height and mandibular length. The second is that ascending ramus height and mandibular length have an important influence on sagittal condylar sliding. The third is that the absolute length of the temporal articular surface has an important influence on relative sagittal sliding.

This study demonstrates the importance of absolute dimensions of the masticatory apparatus as variables that influence the mechanics of jaw motion, particularly rotation. An understanding of both the load-related and the movement-related features of the masticatory apparatus will require an analysis of absolute dimensions in conjunction with mechanically scaled dimensions.

ACKNOWLEDGMENTS

I sincerely thank the people who helped me complete the cineradiographic analysis: Bill Jungers, Marianne Crisci, Jim Harrison, David Reim, Mark Bookbinder, Daniel Schmitt, Rebecca German, Dave Hertweck, Bill Hylander, and Rich Kay. The morphometric work was completed with the help of Bill Stanley (Field Museum of Natural History), Linda Gordon (United States National Museum), Maria Rutzmoser (Museum of Comparative Zoology, Harvard University), and the late Wolfgang Fuchs (American Museum of Natural History). A number of people have read this manuscript either as part of my dissertation or in its present form and have improved it tremendously. I greatly appreciate the comments and criticism of Steve Churchill, Brigitte Demes, John Fleagle, Bill Hylander, Kirk Johnson, Bill Jungers, Dave Krause, Daniel Schmitt, Kathleen Smith, Mark Spencer, and three anonymous reviewers. This research was supported by an NSF graduate fellowship, NSF DBS-9209004 (Jack T. Stern, Susan G. Larson, and William L. Jungers of SUNY Stony Brook), NSF DBS-9215072, and the LSB Leakey Foundation.

LITERATURE CITED

Angel JL. 1948. Factors in temporomandibular joint form. Am J Anat 83:223–245.

Arendsen deWolff-Exalto E. 1951a. On differences in the lower jaw of animalivorous and herbivorous mammals I. Proc Kon Ned Akad v Wetenschapp (Amsterdam) Series C 54:237–246.

Arendsen de Wolff-Exalto E. 1951b. On differences in the lower jaw of animalivorous and herbivorous mammals II. Proc Kon Ned Akad v Wetenschapp (Amsterdam) Series C 54:405–410.

Ashton EH, Zuckerman S. 1954. The anatomy of the articular fossa (fossa mandibularis) in man and apes. Am J Phys Anthropol 12:29–50.

Bennett NG. 1908. A contribution to the study of the movements of the mandible. Proc R Soc Med (Odont Sect) 1(3):79–98.

Bouvier M. 1986a. A biomechanical analysis of scaling in Old World monkeys. Am J Phys Anthropol 69:473–482.

Bouvier M. 1986b. Biomechanical scaling of mandibular dimensions in New World monkeys. Int J Primatol 7:551–567.

Bouvier M, Hylander WL. 1982. The effect of dietary consistency on morphology of the mandibular condylar cartilage in young macaques (*Macaca mulatta*). In: Dixon AD, Sarnat BG, editors. Factors and mechanisms influencing bone growth. New York: Alan R. Liss. p 569–579.

Boyd RL, Gibbs CH, Mahan PE, Richmond AF, Laskin JL. 1990. Temporomandibular joint forces measured at the condyle of *Macaca arctoides*. Am J Orthod Dentofacial Orthop 97:472–479.

Carlson DS. 1977. Condylar translation and the function of the superficial masseter muscle in the rhesus monkey (*M. mulatta*). Am J Phys Anthropol 47:53–63.

Carlson DS, McNamara JA Jr, Jaul DH. 1978. Histological analysis of growth of the mandibular condyle in the rhesus monkey (*Macaca mulatta*). Am J Anat 151:103–118.

Carlson DS, McNamara JA Jr, Graber LW, Hoffman DL. 1980. Experimental studies of growth and adaptation of TMJ. In: Irby WB, editor. Current advances in oral surgery, vol 3. St Louis: Mosby. p 28–77.

Chew CL, Lucas PW, Tay DKL, Keng SB, Ow RKK. 1988. The effect of food texture on the replication of jaw movement during mastication. J Dent 16:210–214.
Cole TM III. 1992. Postnatal heterochrony of the masticatory apparatus in *Cebus apella* and *Cebus albifrons*. J Hum Evol 23:253–282.
Conover WJ, Iman RL. 1981. Rank transformation as a bridge between parametric and nonparametric statistics. Am Stat 35:124–133.
Crompton AW. 1963. The evolution of the mammalian jaw. Evolution 17:431–439.
Crompton AW, Hylander WL. 1986. Changes in mandibular function following the acquisition of a dentary-squamosal articulation. In: Hotton N, MacLean PD, Roth J, Roth EC, editors. The ecology and biology of mammal-like reptiles. Washington, DC: Smithsonian Institution Press. p 263–282.
Davis DD. 1964. The giant panda, a morphological study of evolutionary mechanisms. Fieldiana: Zoology Memoirs 3:1–339.
Diaz-Tay J, Jayasinghe N, Lucas PW, McCallum JC, Jone JT. 1991. Association between surface electromyograms of human jaw-closing muscle and quantified food breakdown. Arch Oral Biol 36:893–898.
DuBrul EL. 1977. Early hominid feeding mechanisms. Am J Phys Anthropol 74:305–320.
Freeman PW. 1988. Frugivorous and animalivorous bats (Microchiroptera): dental and cranial adaptations. Biol J Linn Soc 33:249–272.
Gallo LM, Airoldi GB, Airoldi RL, Palla S. 1997. Description of mandibular finite helical axis pathways in asymptomatic subjects. J Dent Res 76:704–713.
Gibbs CH. 1969. Functional movements of the mandible. Report EDC 4–69–24. Cleveland: Case Western Reserve University. 199 p.
Granados JI. 1979. The influence of the loss of teeth and attrition on the articular eminence. J Prosthet Dent 42:78–85.
Greaves WS. 1978. The jaw lever system in ungulates: a new model. J Zool Lond 184:271–285.
Greaves WS. 1980. The mammalian jaw mechanism—the high glenoid cavity. Am Nat 116:432–440.
Herring SW. 1992. Muscles of mastication: architecture and functional organization. In: Davidovitch Z, editor. The biological mechanisms of tooth movement and craniofacial adaptation. Columbus: Ohio State University College of Dentistry. p 541–548.
Herring SW, Herring SE. 1974. The superficial masseter and gape in mammals. Am Nat 108:561–576.
Hiiemae KM, Kay RF. 1973. Evolutionary trends in the dynamics of primate mastication. In: Zingeser MR, editor. Craniofacial biology of primates, vol 3. Proceedings of the IVth International Conference on Primatology. Basel: Karger. p 28–64.
Hinton RJ. 1981. Changes in articular eminence morphology with dental function. Am J Phys Anthropol 54:439–455.
Humphreys H. 1932. Age changes in the temporomandibular joint and their importance in orthodontics. Int J Orthod Oral Surg Radiog 18:809–815.
Hylander WL. 1975. The human mandible: lever or link? Am J Phys Anthropol 43:227–242.
Hylander WL. 1979a. An experimental analysis of the temporomandibular joint reaction force in macaques. Am J Phys Anthropol 51:433–456.
Hylander WL. 1979b. The functional significance of primate mandibular form. J Morphol 160:223–239.
Hylander WL. 1992. Functional anatomy. In: Sarnat BG, Laskin DM, editors. The temporomandibular joint: a biological basis for clinical practice, 4th ed. Philadelphia: WB Saunders Co. p 60–92.
Hylander WL, Crompton AW. 1980. Loading patterns and jaw movement during the masticatory power stroke in macaques. Am J Phys Anthropol 52:239–251.
Hylander WL, Crompton AW. 1986. Jaw movements and patterns of mandibular bone strain during mastication in the monkey *Macaca fascicularis*. Arch Oral Biol 31:841–848.
Hylander WL, Crompton AW, Johnson KR. 1987. Loading patterns and jaw movements during mastication in *Macaca fascicularis:* a bone-strain, electromyographic, and ineradiographic analysis. Am J Phys Anthropol 72:287–312.
Jablonski NG, Crompton RH. 1994. Feeding behavior, mastication, and tooth wear in the western tarsier (*Tarsius bancanus*). Int J Primatol 15:29–60.
Kay RF. 1975. The functional adaptation of primate molar teeth. Am J Phys Anthropol 43:195–216.
Kay RF, Hiiemae KM. 1974a. Jaw movement and tooth use in recent and fossil primates. Am J Phys Anthropol *40*:227–256.
Kay RF, Hiiemae KM. 1974b. Mastication in *Galago crassicaudatus:* a cinefluorographic and occlusal study. In Martin RD, Doyle GA, Walker AC, editors. Prosimian biology. Pittsburgh: University of Pittsburgh Press. p 501–530.
Keith A. 1894. The ligaments of the catarrhine monkeys, with references to corresponding structures in man. J Anat Phys 28:149–168.
Lebedinsky NG. 1938. Ueber die funktionelle Bedeutung der verschiedenen Höhe des Ramus ascendens mandibulae bezw. des Unterkiefergelenkes bei Säugetieren. Vierteljahrschr Naturf Ges Zürich Suppl 83: 217–224.
Lindblom G. 1960. On the anatomy and function of the temporomandibular joint. Acta Odontol Scand Suppl 28:1–287.
Mack PJ. 1984. A functional explanation for the morphology of the temporomandibular joint of man. J Dent 12:225–230.
Maynard Smith J, Savage RJG. 1959. The mechanics of mammalian jaws. School Sci Rev 141:289–301.
Miller DI, Petak KL. 1973. Three-dimensional cinematography. Kinesiology 3:14–19.
Mills JRE. 1955. Ideal dental occlusion in the primates. Dent Pract 6:57–67.
Mills JRE. 1963. Occlusion and malocclusion in the teeth of primates. In Brothwell DR, editor. Dental anthropology. Oxford: Oxford University Press. p 29–51.
Mills JRE. 1978. The relationship between tooth patterns and jaw movements in the Hominoidea. In: Butler PM, Joysey KA, editors. Development, function and evolution of teeth. New York: Academic Press. p 341–353.
Moffett BC Jr, Johnson LC, McCabe JB, Askew HC. 1964. Articular remodelling in the adult human temporomandibular joint. Am J Anat 115:119–142.
Moore WJ. 1981. The mammalian skull. Cambridge: Cambridge University Press. p 159–161.
Nickel JC, McLachlan KR, Smith DM. 1988a. Eminence development of the postnatal human temporomandibular joint. J Dent Res 67:896–902.
Nickel JC, McLachlann KR, Smith DM. 1988b. A theoretical model of loading and eminence development of the postnatal human temporomandibular joint. J Dent Res 67:903–910.
Oberg T, Carlsson GE, Fajers CM. 1971. The temporomandibular joint. A morphologic study of human autopsy material. Acta Odontol Scand 29:349–384.
Osborn JW. 1989. The temporomandibular ligament and the articular eminence as constraints during jaw opening. J Oral Rehabil 16:323–333.

Panjabi MM. 1979. Centers and angles of rotation of body joints: A study of errors and optimization. J Biomech 12:911–920.
Parsons FG. 1900. The joints of mammals compared with those of man: a course of lectures delivered at the Royal College of Surgeons of England. J Anat Phys 34:41–68.
Picq PG. 1990. L'articulation temporo-mandibulaire des homidés. Biomécanique, allométrie, anatomie comparée et évolution. Paris: Cahiers de Paléoanthropologie, Editions du CNRS.
Postic SD, Teodosijevic MV, Krstic MS. 1991. Graphic assessment of interincisal point movements during chewing of hard and soft foods. Quint Int 22:623–630.
Rees LA. 1954. The structure and function of the mandibular joint. Br Dent J 96:125–133.
Robinson JT. 1952. The australopithecines and their evolutionary significance. Proc Linn Soc Lond 163:194–204.
SAS Institute Inc. (1985) Version 5. Cary, NC: Statistical Analysis Software, Inc.
SAS Institute, Inc. (1988) SAS-pc release 6.03. Cary, NC: Statistical Analysis Software, Inc.
Schmolke C. 1990. The relationship between the temporomandibular joint capsule, articular disc and jaw muscles. J Anat 184:335–345.
Sheppard IM. 1962. Anteroposterior and posteroanterior movements of the mandible and condylar centricity during function. J Prosthet Dent 12:86–94.
Sicher H. 1948. Some aspects of the anatomy and pathology of the temporomandibular articulation. Bur 47:14–36.
Smith RJ. 1978. Mandibular biomechanics and temporomandibular joint function in primates. Am J Phys Anthropol 49:341–350.
Smith RJ, Jungers WL. 1997. Body mass in comparative primatology. J Hum Evol 32:523–559.
Sokal RR, Rohlf FJ. 1981. Biometry, 2nd ed. New York: W. H. Freeman and Co.
Teaford MF, Oyen OJ. 1989. In vivo and in vitro turnover in dental microwear. Am J Phys Anthropol 80:447–460.
Todd TW. 1930. Facial growth and mandibular adjustment. Int J Orthod Oral Surg Radiog 16:1243–1272.
Wall CE. 1995. Form and function of the temporomandibular joint in anthropoid primates. PhD dissertation, State University of New York at Stony Brook, Stony Brook, NY.
Wall CE. 1997. The expanded mandibular condyle of the Megaladapidae. Am J Phys Anthropol 103:263–276.
Ward SC, Molnar S. 1980. Experimental stress analysis of topographic diversity in early hominid gnathic morphology. Am J Phys Anthropol 53:383–395.
Warwick James W. 1960. The jaws and teeth of primates. London: Pitman Medical Publishing Co. p 301–304.
Weijs WA, van Ruijven LJ. 1990. Models of masticatory mechanics: their reliability, resolving power and usefulness in functional morphology. Neth J Zool 40:136–152.
Weijs WA, Korfage JAM, Langenbach GJ. 1989. The functional significance of the position of the centre of rotation for jaw opening and closing in the rabbit. J Anat 162:133–148.